MNRAS **000**, 1–9 (2015) Preprint 24 September 2015 Compiled using MNRAS LATEX style file v3.0

Ellicular galaxies and their (non over-massive) black holes

Giulia A. D. Savorgnan[1]⋆, Alister W. Graham[1]

[1] *Centre for Astrophysics and Supercomputing, Swinburne University of Technology, Hawthorn, Victoria 3122, Australia.*

24 September 2015

ABSTRACT

The classification "early-type" galaxy includes both elliptically- and lenticular-shaped galaxies, with the latter composed of a spheroidal stellar system encased within a larger, but flatter, stellar disc. Theoretically, the spheroid-to-disc flux ratio can assume any positive value, but in practice studies often consider only spheroid/disc decompositions in which the disc neatly dominates over the spheroid at large galaxy radii, creating an inner "bulge" as observed in most spiral galaxies. Here we reveal that decompositions in which the disc remains embedded within the spheroid, labelled by some as "unphysical", correctly reproduce both the photometric and kinematic properties of a class of early-type galaxy intermediate between that of elliptical and lenticular galaxies, which we refer to as *ellicular* galaxies for ease of reference. Ellicular galaxies have often been confused with lenticular galaxies, such that their spheroid luminosities have been considerably underestimated. This has recently led to some surprising conclusions, such as the claim that a number of ellicular galaxies (e.g. Mrk 1216, NGC 1277, NGC 1271, and NGC 1332) host a central black hole whose mass is abnormally large compared to expectations from the (underestimated) spheroid luminosity. We show that when ellicular galaxies are correctly modelled, they no longer appear as extreme outliers in the (black hole mass)-(spheroid mass) diagram. This not only nullifies the need for invoking different evolutionary scenarios for these galaxies but it strengthens the significance of the observed (black hole mass)-(spheroid mass) correlation and confirms its importance as a fundamental ingredient for theoretical and semi-analytic models used to describe the coevolution of spheroids and their central supermassive black holes.

Key words: galaxies: classification – galaxies: bulges – galaxies: elliptical and lenticular, cD – galaxies: evolution – galaxies: structure – galaxies: individual: Mrk 1216, NGC 1271, NGC 1277, NGC 1332, NGC 4291

1 INTRODUCTION

There are currently two well-known types of stellar discs in galaxies. The first are the large-scale discs (with exponential scale lengths of a few kiloparsec) that dominate the light at large radii in spiral and lenticular galaxies; the second are the small (tens to a couple of hundred parsec) nuclear discs observed in both early- and late-type galaxies (e.g. Scorza & van den Bosch 1998; Rest et al. 2001; Balcells et al. 2007; Ledo et al. 2010). The origin of the nuclear discs has been speculated to arise from the infall of small satellite galaxies or gas clouds. The origin, or at least the on-going feeding and growth, of the large-scale discs has been attributed to cold gas flows, gas rich mergers and halo accretion events (e.g. White & Rees 1978; White & Frenk 1991; Navarro & Benz 1991; Barnes & Hernquist 1992; Khochfar & Silk 2006; Dekel et al. 2009; Ceverino et al. 2010, 2012; Conselice et al. 2012; Rubin et al. 2012; Martini et al. 2013; Ueda et al. 2014), and a thorough review can be found in Combes (2014a,b). On the other hand, intermediate-sized discs have not received the same level of attention as their nuclear and large-scale homologues and they have at times been labelled and rejected as "unphysical" when detected. Here we focus on the increasingly overlooked occurence of intermediate-scale discs in galaxies with directly measured black hole masses. We report on the photometric and kinematical signatures of these intermediate-sized stellar discs, and the impact they have on the (black hole mass)-to-(spheroid stellar mass) ratio which is used to constrain galaxy evolution models.

The majority of stellar discs have some level of inclination with respect to our line-of-sight, and this makes them ap-

⋆ E-mail: gsavorgn@astro.swin.edu.au

pear elliptical (rather than round) when seen in projection on the sky. This can help one distinguish them from the more spherically-shaped spheroids. Identifying the radial extent of these discs with respect to the spheroid can however be subtle. Two-dimensional kinematic maps represent an important diagnostic tool for this purpose. Most early-type galaxies are classified as "central fast rotators" (Franx et al. 1989; Emsellem et al. 2011; Scott et al. 2014), that is, they are rapidly rotating within their half-light radius. However, more extended kinematic maps (Arnold et al. 2014) reveal that some of the central fast rotators continue to be fast rotating at large radii, whereas other central fast rotators become slow rotators in their outer regions. A specific angular momentum profile that is rapidly increasing beyond 1–2 half-light radii is a signature of a large-scale disc, while a specific angular momentum profile that increases up to 1–2 half-light radii and then declines beyond that point indicates the presence of an intermediate-scale disc that no longer dominates at large radii. Unfortunately, such extended kinematic maps are not yet available for large numbers of galaxies in the local Universe. Nevertheless, the ellipticity profile of a galaxy's isophotes can help identify the extent of stellar discs in early-type galaxies.

Building on the investigation of Rix & White (1990), the toy model shown in Figure 1 illustrates the typical ellipticity profile ($\epsilon = 1 - b/a$, where b/a is the ratio of minor-to-major axis length) of (i) a "lenticular" galaxy comprised of a large-scale disc which dominates the light at large radii over a relatively smaller encased bulge, (ii) an "elliptical" galaxy with an additional nuclear stellar disc, and (iii) a galaxy composed of an intermediate-scale disc embedded in a relatively larger spheroid which dominates the light at large radii. We refer to the last case as an "ellicular" galaxy. In general, stellar discs are intrinsically flat and circular; their ellipticity, dictated by their inclination to our line of sight, is fixed. Spheroids are often rounder than the observed projection on the sky of their associated discs, thus their average ellipticity is often lower than that of their disc. An ellipticity profile that increases with radius can be ascribed to an inclined disc that becomes progressively more important at large radii, whereas a radial decrease of ellipticity signifies the opposite case. This approach can be taken to the next level by inspecting the isophotes for discy structures and checking the velocity line profiles for asymmetry (e.g. Scorza & Bender 1995 and references therein; Scorza 1998).

The awareness that many so-called "elliptical" galaxies actually contain stellar discs dates back many years (Michard 1984; Djorgovski 1985; Carter 1987; Capaccioli 1987; Capaccioli et al. 1988; Franx et al. 1989; Nieto et al. 1988, 1991; Rix & White 1990, 1992; van den Bergh 1990; Bender 1990; Scorza & Bender 1990, 1995; Simien & Michard 1990; Cinzano & van der Marel 1993; D'Onofrio et al. 1995; Graham et al. 1998; Scorza 1998; Scorza & van den Bosch 1998; Bender & Saglia 1999) and, more recently, intermediate-scale discs were anything but unfamiliar to Kormendy & Bender (2012) and Krajnović et al. (2013). However, the class of ellicular galaxies has been missed by many galaxy modellers of late, who have labelled as "unphysical" (Allen et al. 2006) those spheroid/disc decompositions in which the disc does not dominate over the spheroid at large radii as is observed with spiral galaxies. Indeed, Graham et al. (2011, his Figure 7) warned about such erroneous fits to spiral galaxies. This bias has led to the rejection of many early-type galaxy decompositions similar to that illustrated in the middle panel of Figure 1. Unsurprisingly, studies affected by this bias have not obtained spheroid/disc decompositions with a spheroid-to-total ratio larger than $0.6 - 0.8$ (e.g. Gadotti 2008; Head et al. 2014; Querejeta et al. 2015; Méndez-Abreu & CALIFA Team 2015). In this paper we investigate the influence this has had on research pertaining to supermassive black hole mass scaling relations involving the host spheroid.

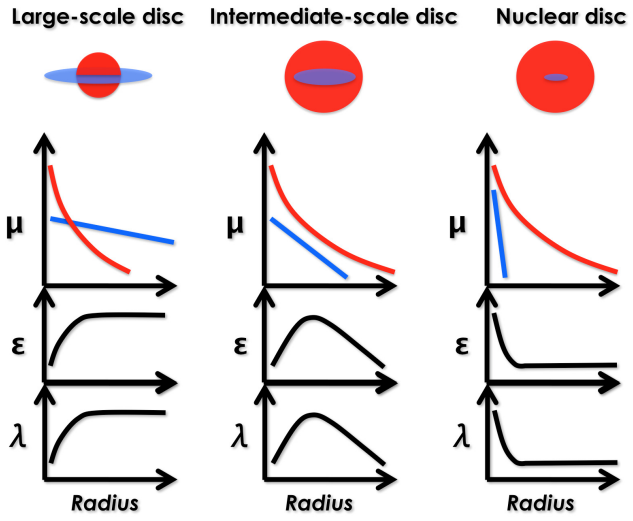

Figure 1. Illustration of the spheroid/disc decomposition of the one-dimensional surface brightness profile, μ, the ellipticity profile, ϵ, and the specific angular momentum profile, λ, for the three prototype early-type galaxy sub-classes. In the flux decompositions, the spheroid (or bulge) and the disc are shown with the red and blue color, respectively. The left panel shows a lenticular galaxy, composed of a bulge encased in a large-scale disc. The right panel displays an elliptical galaxy with (an optional) nuclear stellar disc. The middle panel presents an early-type galaxy with an intermediate-sized disc embedded in the spheroid. We refer to the last case as an ellicular galaxy.

This paper is structured as follows. In Section 2 we present a detailed photometric analysis of three ellicular galaxies (Mrk 1216, NGC 1332, and NGC 3115) and we briefly describe another five ellicular galaxies (NGC 821, NGC 1271, NGC 1277, NGC 3377, and NGC 4697) already modelled by us elsewhere in the literature. We compare our photometric analysis with the kinematical information available from the literature, and explain the differences between our galaxy models and past decompositions. In Section 3 we explore the important implications this has for the (black hole mass)-(spheroid stellar mass) diagram. In Section 4 we discuss our results in terms of galaxy evolution and we present the location of ellicular galaxies, relative to other galaxies, in the Hubble grid.

2 INTERMEDIATE-SCALE DISC GALAXIES

Three examples of ellicular galaxies are Mrk 1216, NGC 1332, and NGC 3115. In the following Sections, we present a photometric analysis of these three galaxies, and we com-

pare our results with the kinematical analysis available from the literature for Mrk 1216 and NGC 3115. For the galaxies NGC 1332 and NGC 3115, we used 3.6 μm images obtained with the InfraRed Array Camera (IRAC) onboard the *Spitzer Space Telescope*. For the galaxy Mrk 1216, we used an archived Hubble Space Telescope (*HST*) image taken with the Wide Field Camera 3 (WFC3) and the near-infrared *F160W* filter (*H*-band). Our galaxy decomposition technique is extensively described in Savorgnan & Graham (2015). Briefly, the galaxy images were background-subtracted, and masks for contaminating sources were created. The one-dimensional Point Spread Function (PSF) was characterized using a Gaussian profile for the *HST* observation and a Moffat (1969) profile for the *Spitzer* observations. We performed an isophotal analysis of the galaxies using the IRAF[1] task `ellipse`[2] (Jedrzejewski 1987). The galaxy isophotes were modelled with a series of concentric ellipses, allowing the ellipticity, the position angle and the amplitude of the fourth harmonic to vary with radius. The decomposition of the surface brightness profiles was performed with software written by G. Savorgnan and described in Savorgnan & Graham (2015). We modelled the light profiles with a combination of PSF-convolved analytic functions, using one function per galaxy component.

2.1 NGC 3115

The presence of a disc in NGC 3115 is obvious due to its edge-on orientation (Figure 2). Less obvious is the radial extent of this disc, if one only relies on a visual inspection of the galaxy image. The ellipticity profile (Figure 2) is consistent with the presence of an intermediate-scale disc. Moreover, the kinematics of NGC 3115 (Arnold et al. 2011) also disprove the presence of a large-scale disc, because the galaxy is rapidly rotating only within two galaxy half-light radii ($\sim 2 \times 50$ arcsec), and the rotation significantly drops at larger radii. The unsharp mask of NGC 3115 (Figure 2) betrays the presence of a faint edge-on nuclear ring, which can also be spotted as a small peak in the ellipticity profile (at semi-major axis length $R_{\rm maj} \sim 15$ arcsec). Such rings are common in early-type galaxies (Michard & Marchal 1993). The spheroidal component of NGC 3115 is well described with a Sérsic (1963) profile. The highly inclined intermediate-scale disc is better fit with an $n < 1$ Sérsic profile (the Sérsic index n regulates the curvature of the Sérsic profile) rather than with an exponential function, as explained by Pastrav et al. (2013). The nuclear ring is modelled with a Gaussian function.
In comparison, Läsker et al. (2014a) fit NGC 3115 with a bulge + disc + envelope, and measured a bulge half-light radius of 3.9 arcsec and a bulge-to-total ratio of 0.12. We describe this galaxy using a spheroid + intermediate-scale disc + nuclear ring, and obtain a spheroid half-light radius of 43.6 arcsec and a spheroid-to-total ratio of 0.85. We have used both kinematical information and ellipticity profiles, together with the surface brightness profile, to obtain a physically consistent and meaningful model.

2.2 NGC 1332

The morphology of NGC 1332 (Figure 3) is very similar to that of NGC 3115, with the ellipticity profile indicating the presence of an intermediate-scale disc, although in this case no nuclear component is evident. We were not able to find any extended kinematic profile or map for this galaxy in the literature. The data within the innermost 6 arcsec were excluded from the fit because, according to our galaxy decomposition, they are possibly affected by the presence of a partially depleted core. The surface brightness profile of NGC 1332 is well described with a Sérsic-spheroid plus an $n < 1$ Sérsic-disc. Our galaxy decomposition suggests that NGC 1332 is a spheroid-dominated galaxy, with a spheroid-to-total ratio of 0.95.
Rusli et al. (2011) did not identify the restricted extent of the intermediate-scale disc, as revealed by the ellipticity profile, and proposed a model featuring a Sérsic-bulge and a large-scale exponential-disc, with a spheroid-to-total ratio of 0.43. Based on their bulge/disc decomposition, they concluded that NGC 1332 is a disc-dominated lenticular galaxy which is displaced from the (black hole mass)-(spheroid luminosity) correlation of Marconi & Hunt (2003) by an order of magnitude along the black hole mass direction. However, in Section 3 we show that, according to our decomposition, NGC 1332 lies within the 1σ scatter about the (black hole mass)-(spheroid stellar mass) correlation for early-type galaxies. We also note that the majority of galaxies with an elevated stellar velocity dispersion ($\sigma > 270$ km s^{-1}) are core-Sérsic galaxies (Graham et al. 2003; Ferrarese et al. 2006; Dullo & Graham 2014), i.e. they have a partially depleted core which has been identified from high-resolution photometric data. NGC 1332 has $\sigma = 320$ km s^{-1}, but, based on their decomposition of *HST* imaging, Rusli et al. (2011) did not find a core in this galaxy. However, our galaxy decomposition (Figure 3) suggests that NGC 1332 is in fact a core-Sérsic galaxy. Since we did not use high-resolution photometric data, we refrain from a firm conclusion, but we caution that a re-analysis of the *HST* data – by taking into account the correct radial extent of the intermediate-scale disc – may indeed reveal the presence of a depleted core in this galaxy.

2.3 Mrk 1216

Although the disc in the galaxy Mrk 1216 is not immediately apparent from the image (Figure 4), the velocity map (Yıldırım et al. 2015) reveals the presence of a

[1] IRAF is the Image Reduction and Analysis Facility, distributed by the National Optical Astronomy Observatory, which is operated by the Association of Universities for Research in Astronomy (AURA) under cooperative agreement with the National Science Foundation.
[2] Our analysis was performed before `isofit` (Ciambur 2015) was conceived or available. After `isofit` was recently developed and implemented in IRAF, we employed it to re-extract the surface brightness profiles of the galaxies NGC 1332 and NGC 3115. We then repeated the analysis and checked that this change does not significantly alter our results. In fact, although `isofit` provides a more accurate description of the isophotes in the presence of an inclined disc, the discs of NGC 1332 and NGC 3115 are relatively faint compared to the spheroidal components, therefore the differences between the light profile obtained with `ellipse` and that obtained with `isofit` are small for these two galaxies.

fast rotating component within three galaxy half-light radii ($\sim 3 \times 5$ arcsec). The ellipticity profile (Figure 4), which extends out to five half-light radii, indicates the presence of an intermediate-scale disc. In addition, a nuclear disc is identified from the change in slope of the ellipticity profile ($R_{\rm maj} \sim 1-2$ arcsec), from the unsharp mask, and from a clear feature in the $B4$ fourth harmonic profile (not shown here). We modelled the surface brightness profile of Mrk 1216 (Figure 4) with a Sérsic-spheroid, an intermediate-sized exponential-disc, and a nuclear exponential-disc.

2.4 Other galaxies

Our models with an intermediate-sized disc embedded within a larger spheroidal component, plus an additional nuclear component when one is present, match the observed light distribution, and explain both the extended kinematic maps (when available, Arnold et al. 2014) and the ellipticity profiles, of five additional galaxies for which a direct measurement of their central supermassive black hole mass is available: NGC 821; NGC 1271; NGC 1277; NGC 3377; and NGC 4697. Our isophotal analysis and galaxy decompositions for NGC 1271 and NGC 1277 will be presented in Graham, Savorgnan & Ciambur (*in prep.*) and Graham et al. (2015), respectively, while the galaxies NGC 821, NGC 3377 and NGC 4697 have been analysed in Savorgnan & Graham (2015).

2.4.1 NGC 1271

Walsh et al. (2015) explored a three-component decomposition for NGC 1271 and identified the galaxy bulge with the innermost of the three components, having a half-light radius of 0.61 arcsec and a bulge-to-total flux ratio of 0.23; our model features a spheroid + intermediate-scale disc, with a spheroid half-light radius of 3.3 arcsec and a spheroid-to-total flux ratio of 0.67.

2.4.2 NGC 1277

van den Bosch et al. (2012) proposed a model for the galaxy NGC 1277 with a bulge + disc + nuclear source + envelope, which gives a bulge half-light radius of 0.9 arcsec and a bulge-to-total flux ratio of 0.24; our model consists of a spheroid + intermediate-scale disc + nuclear component, and produces a spheroid half-light radius of 6.0 arcsec and a spheroid-to-total flux ratio of 0.79.

2.4.3 NGC 3377

Läsker et al. (2014a) modelled the galaxy NGC 3377 with a bulge + nuclear disc + disc + envelope, and obtained a bulge half-light radius of 10.1 arcsec and a bulge-to-total flux ratio of 0.35; our model with a spheroid + intermediate-scale disc + nuclear disc returns a spheroid half-light radius of 61.8 arcsec and a spheroid-to-total flux ratio of 0.94.

2.4.4 NGC 821

Läsker et al. (2014a) decomposed the galaxy NGC 821 into a bulge + disc + envelope, and measured a bulge half-light radius of 3.8 arcsec and a bulge-to-total flux ratio of 0.19; our decomposition consists of a spheroid + intermediate-scale disc, with a spheroid half-light radius of 36.5 arcsec and a spheroid-to-total flux ratio of 0.79.

2.4.5 NGC 4697

The galaxy NGC 4697 represents an "extreme" case. Läsker et al. (2014a) fit this galaxy with a bulge + nuclear source + disc + envelope, and obtained a bulge half-light radius of 6.3 arcsec and a bulge-to-total flux ratio of 0.08; we described NGC 4697 using a spheroid + intermediate-scale disc + nuclear disc model, and measured a spheroid half-light radius of 239.3 arcsec and a spheroid-to-total flux ratio of 0.89.

Past models that "forcedly" described ellicular galaxies using an inner bulge encased within a large-scale disc commonly required the addition of an extended envelope or halo to account for the outer portion of the spheroid. Such three-component models (bulge + disc + envelope) typically reduce the spheroid luminosity by a factor of $3-4$, and underestimate the size of the spheroid by a factor of $6-10$, although more "extreme" cases can be found.

3 THE BLACK HOLE – SPHEROID CORRELATION

Inaccurate measurements of the spheroid-to-total ratio of galaxies can impact galaxy scaling relations. Recently, a handful of ellicular galaxies have been claimed to host *over-massive* black holes, i.e. the mass of their central supermassive black hole has been reported to be significantly larger than what is expected from the galaxy's spheroid luminosity (or stellar mass). This is the case for the galaxies Mrk 1216 (for which only an upper limit on its black hole mass has been published, Yıldırım et al. 2015), NGC 1271 (Walsh et al. 2015), NGC 1277 (van den Bosch et al. 2012; Yıldırım et al. 2015) and NGC 1332 (Rusli et al. 2011). In addition to these, the elliptical galaxy NGC 4291 has also been claimed to be a $\sim 3.6\sigma$ outlier above the (black hole mass)-(spheroid mass) scaling relation (Bogdán et al. 2012). Obviously, having both the black hole mass and the spheroid mass correct is important for placing systems in the (black hole mass)-(spheroid mass) diagram.

At present, for early-type galaxies, the spheroid luminosity and the galaxy luminosity can be used to predict the black hole mass with the same level of accuracy[3] *(Savorgnan et al. 2015). If a galaxy hosts a black hole that is over-massive compared to expectations from the spheroid luminosity, but whose mass is normal compared to expectations from the*

[3] Note that Läsker et al. (2014b) reported that the spheroid luminosity and the galaxy luminosity are equally good tracers of the black hole mass irrespective of the galaxy morphological type, but their sample of 35 galaxies contained only 4 spiral galaxies. However, using a sample of 45 early-type and 17 spiral galaxies, Savorgnan et al. (2015) shows that, when considering all galaxies irrespective of their morphological type, the correlation of the black hole mass with the spheroid luminosity is better than that with the galaxy luminosity.

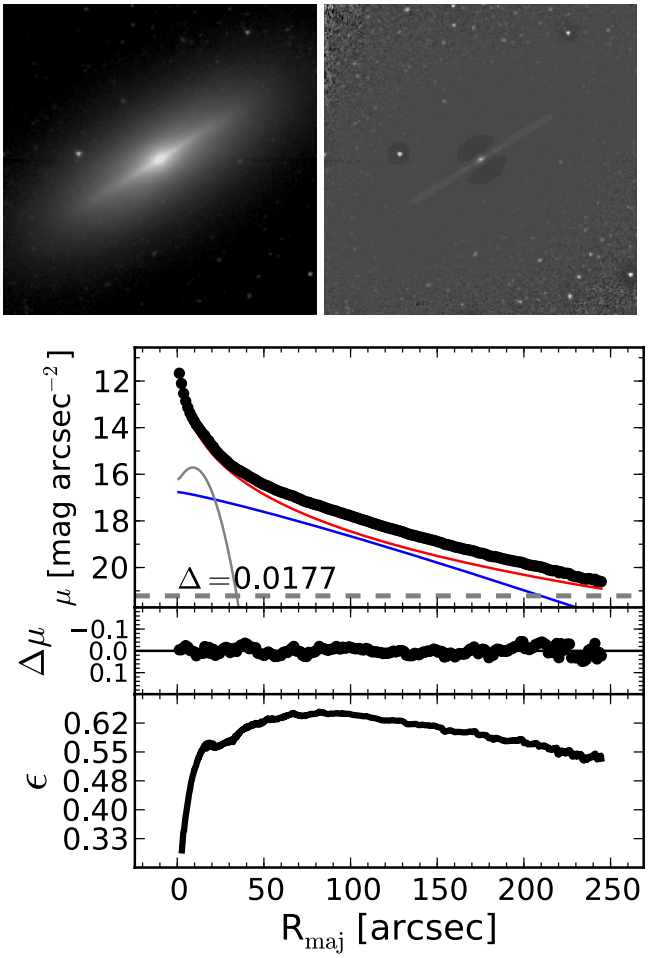

Figure 2. NGC 3115. The top panels are the *Spitzer*/IRAC 3.6 μm image (left) and its unsharp mask (right), obtained by dividing the image by a Gaussian-smoothed version of itself. The bottom plots display the best-fit model of the surface brightness profile, μ, and the ellipticity profile, ϵ, along the major-axis, $R_{\rm maj}$. The black points are the observed data, which extend out to five galaxy half-light radii ($\sim 5 \times 50$ arcsec). The color lines represent the individual (PSF-convolved) model components: red = Sérsic (spheroid), blue = Sérsic (disc), gray = Gaussian ring. The residual profile (data − model) is shown as $\Delta\mu$. The horizontal gray dashed line corresponds to an intensity equal to three times the root mean square of the sky background fluctuations. Δ denotes the root mean square scatter of the fit in units of mag arcsec^{-2}.

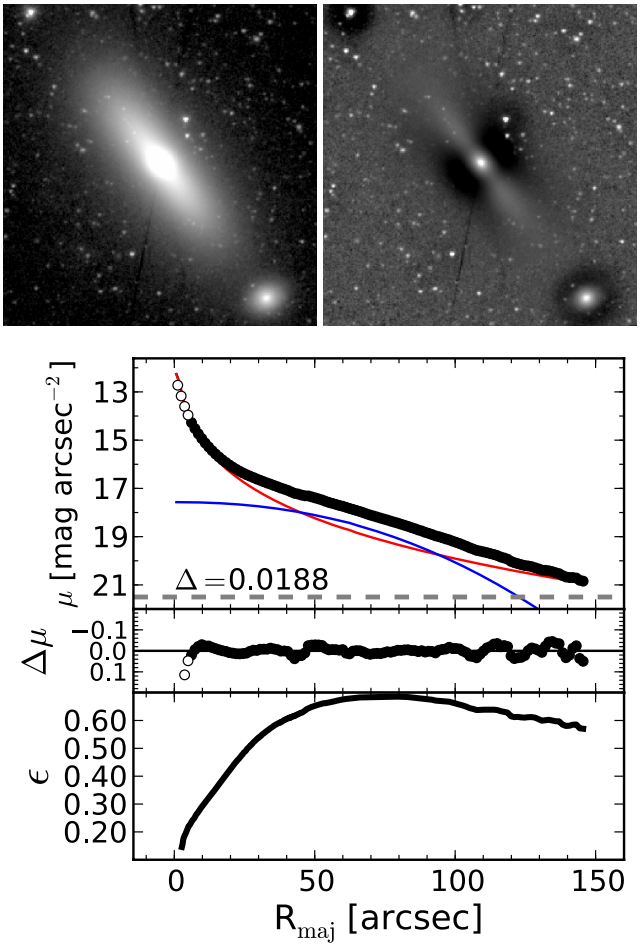

Figure 3. NGC 1332. Same as Figure 2, except for the following. The surface brightness profile extends out to seven galaxy half-light radii ($\sim 7 \times 20$ arcsec). The empty points are data excluded from the fit.

galaxy luminosity, one should wonder whether the spheroid luminosity might have been underestimated due to an inaccurate spheroid/disc decomposition. Indeed, none of the five galaxies just mentioned (Mrk 1216, NGC 1271, NGC 1277, NGC 1332, and NGC 4291) is a noticeable outlier in the (black hole mass)-(galaxy luminosity) diagram. In Figure 5 we show the location of these five galaxies in the updated (black hole mass)-(spheroid stellar mass) diagram for early-type galaxies from Savorgnan et al. (2015). Figure 5 was populated using the galaxy decomposition technique shown here and extensively described in Savorgnan & Graham (2015). Briefly, we obtained Spitzer/IRAC 3.6 μm images for 45 early-type galaxies which already had a dynamical detection of their black hole mass. We modelled their one-dimensional surface brightness profiles with a combination of analytic functions, using one function per galaxy component. Spheroid luminosities were converted into stellar masses using individual, but almost constant mass-to-light ratios ($\sim$0.6, Meidt et al. 2014).

In Figure 5, we show the galaxies Mrk 1216, NGC 1271 and NGC 1277, which were not a part of the original sample of 45 early-type galaxies. For the galaxy NGC 1271, we use the black hole mass measurement and the stellar mass-to-light ratio obtained by Walsh et al. (2015). For the galaxy NGC 1277, we use the black hole mass measurement obtained by van den Bosch et al. (2012) and the stellar mass-to-light ratio obtained by Martín-Navarro et al. (2015). For the galaxy Mrk 1216, we use the upper limit on the black hole mass and the stellar mass-to-light ratio obtained by Yıldırım et al. (2015). For the first time, Figure 5 reveals that when the four ellicular galaxies Mrk 1216, NGC 1271, NGC 1277, NGC 1332, and the elliptical galaxy NGC 4291 are properly modelled, they no longer appear as extreme outliers above the (black hole mass)-(spheroid stellar mass)

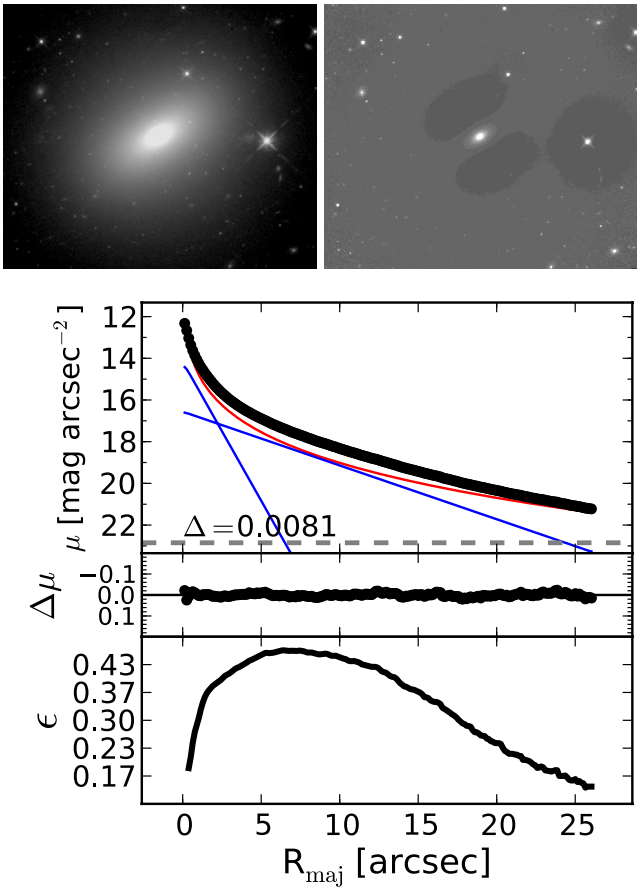

Figure 4. Mrk 1216. Same as Figure 2, except for the following. The top panels are the *HST*/WFC3 *F160W* image (left) and its unsharp mask (right). The surface brightness profile extends out to five galaxy half-light radii ($\sim 5 \times 5$ arcsec). The color lines represent the individual (PSF-convolved) model components: red = Sérsic (spheroid), blue = exponential (disc).

correlation for early-type galaxies, i.e. they all reside well within a 3σ deviation from the correlation.

4 DISCUSSION

4.1 Origin of compact massive galaxies

Acknowledging the correct structure of ellicular galaxies is important to properly understand their origin. According to the current paradigm of cosmological structure evolution, the genesis of massive early-type galaxies is characterized by two distinct phases: "in-situ" and "ex-situ". The first phase takes place in a young Universe (within its first 4 Gyr), when cold gas inflows produced short and intense bursts of star formation that created compact and dense conglomerates of stars with high velocity dispersion (e.g. Prieto et al. 2013). These naked and compact conglomerates, named "red nuggets" (Damjanov et al. 2009), have been observed at high-redshift with half-light sizes of 1–2 kpc (Daddi et al. 2005; Trujillo et al. 2006; van Dokkum et al. 2008). In the second phase (last 10 Gyr), discs and stellar envelopes were accreted around these primordial conglomerates and the external parts of today's galaxies assembled on scales of 2–20 kpc (e.g. Driver et al. 2013).

Today's Universe is populated by an abundance of compact, massive spheroids, with the same physical properties – mass and compactness – as the high-redshift red nuggets (Graham 2013; Graham et al. 2015). Some of these local compact massive spheroids are encased within a large-scale disc, that is to say they are the bulges of some lenticular and spiral galaxies. Over the last 10 Gyr their spheroids have evolved by growing a relatively flat disc (e.g. Pichon et al. 2011; Danovich et al. 2012; Stewart et al. 2013) – rather than a three-dimensional envelope – which has increased the galaxy size but preserved the bulge compactness. The other compact massive spheroids of today's Universe belong to some ellicular galaxies. Indeed, Mrk 1216, NGC 1271, NGC 1277, NGC 1332, and NGC 3115 are all local compact ellicular galaxies with purely old (> 10 Gyr) stellar populations. These galaxies have undergone the lowest degree of disc growth.

In addition to the observational clues as to the actual physical components in ellicular galaxies, one can reason on other grounds as to why these compact galaxies are not comprised of an inner bulge plus large-scale disc plus outer envelope. If they were such three-component systems, then one would have two possibilities. The first possibility is that these galaxies were already fully assembled 10 Gyr ago; this would explain their old stellar populations, but it would also imply that their discs and envelopes had already formed during the first 4 Gyr of the Universe, in disagreement with the current cosmological picture. The second possibility is that only their inner bulges (with sizes of 0.1–0.2 kpc, according to past decompositions) originated in the first 4 Gyr and they subsequently accreted a substantial disc and envelope. If this was correct, then we would observe high-redshift, star-like, naked bulges with stellar masses within a factor of a few times the currently observed red nuggets but sizes which are 10 times smaller. However, a dramatically different expectation is reached if one considers these galaxies today as spheroid-dominated systems with an intermediate-scale disc; in this case, both the galaxy size and the spheroid size are compact (1–2 kpc). This implies that, among the local descendants of the high-redshift red nuggets, the compact ellicular galaxies have undergone the lowest degree of disc growth. That is, the bulk of a compact ellicular galaxy quickly assembled "in-situ" in a very young Universe and experienced very little evolution over the last 10 Gyr.

4.2 Ellicular galaxies in the Hubble grid

The existence of the oft-overlooked, intermediate-scale discs exposes a likely continuum of disc sizes in early-type galaxies, as opposed to a dichotomy of nuclear discs versus large-scale discs. The presence of these intermediate-scale discs also blurs the distinction between elliptical (E) and lenticular (S0: $\epsilon = 1-b/a > 0.7$, Hubble 1936; Sandage 1961) galaxies and arguably creates the need for a new subclass which bridges this divide. While expanding the galaxy nomenclature beyond ellipticals with possible nuclear discs, and lenticulars with large-scale discs, to include something like *elliculars* with intermediate-scale discs will be helpful for distinguishing among early-type galaxies with different disc

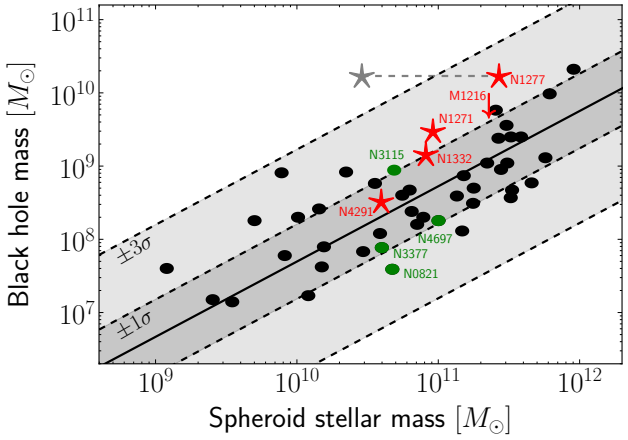

Figure 5. Black hole mass plotted against spheroid stellar mass for 45+3 early-type galaxies (from Savorgnan et al. 2015). The black solid line is the bisector linear regression for all galaxies except Mrk 1216, NGC 1271 and NGC 1277. The dashed lines mark the 1σ and 3σ deviations, where σ (0.51 dex) is the total *rms* scatter about the correlation in the black hole mass direction. The red symbols mark five galaxies that were claimed to be extreme outliers in this diagram: four intermediate-scale disc galaxies (Mrk 1216, NGC 1271, NGC 1277 and NGC 1332) and one elliptical galaxy (NGC 4291). All five reside well within a 3σ deviation from the correlation when using their correct spheroid mass. For NGC 1277, we show the previously reported spheroid stellar mass (van den Bosch et al. 2012) in gray. The green color is used to show the location of four additional intermediate-scale disc galaxies mentioned in Section 2.

[h]

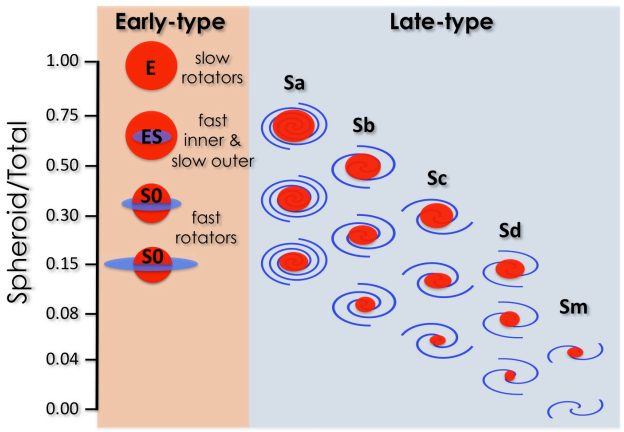

Figure 6. The Hubble grid (Graham 2014), which uses the mean pitch angle of the arms in spiral galaxies to define their morphological type. Ellicular (ES) galaxies are intermediate between elliptical (E) and lenticular (S0) galaxies.

scale-lengths, it should be remembered that just as portions of the electromagnetic spectrum are labelled according to their different wavelengths, there is still an underlying continuum. Similarly, binning early-type galaxies as either a fast-rotator (FR) or a slow-rotator (SR) can hide the fact that a continuum exists. Importantly, in the case of early-type galaxies with intermediate-scale discs, this particular rotation-based classification depends on the galaxy's radial range probed, changing from FR to SR as the radial extent is sufficiently increased. There is thus a need for more than two bins (E vs. S0, or FR vs. SR) and a continuum in the (Hubble-Jeans)-like classification schemes (van den Bergh 1997; Sandage 2005).

It has been argued that the classification scheme for "elliptical" galaxies should not be their apparent axis ratio as seen on the plane of the sky (E0–E7), because this depends on the viewing angle rather than being intrinsic to the galaxy. Obviously when dealing with intermediate-scale discs, the boxy/discy shape of the isophotes is a function of both radius and disc inclination, making a single isophote shape parameter problematic and particularly inappropriate for the classification task at hand. Section 4 of Kormendy & Bender (1996) points out additional complications. Instead, early-type galaxies would be better quantified by their spheroid-to-total flux ratio, with a continuum from pure elliptical galaxies to disc-dominated lenticular galaxies (Figure 6).

While spiral galaxies display a range of spheroid-to-total flux ratios from 0 to ∼3/4 (e.g. Graham & Worley 2008, and references therein), lenticular galaxies typically display a range from ∼3/4 to ∼0.1 (Laurikainen et al. 2010). This spheroid-to-total flux ratio is widely recognised as an important quantity, and its broad range observed in lenticular galaxies recently led to a re-introduction of van den Bergh's (1976) Hubble comb, in which both late-type galaxies (i.e. spiral galaxies) and lenticular galaxies form separate arms of an expanded Hubble-Jeans tuning fork, with an additional arm for disc galaxies hosting anaemic spiral patterns (Cappellari et al. 2011; Kormendy & Bender 2012). However because every spiral Hubble type (e.g. Sa, Sb, Sc), not just the S0 galaxies, has a broad range of spheroid-to-total ratio, and because this information is not captured by the Hubble comb, a grid of spiral morphological type (predominantly determined by the spiral arms) versus spheroid-to-total ratio can also be useful for classifying galaxies.

In Figure 6 we show the location of galaxies with intermediate-scale discs in such a "Hubble grid", which is effectively the quantitative scheme used by Boroson (1981), Kent (1985), Kodaira et al. (1986), Simien & de Vaucouleurs (1986) in which each galaxy type displays a range of spheroid-to-total flux ratio. Rather than a scheme in which the morphological type (a, b, c, etc.) changes if the spheroid-to-total ratio changes – as in the Hubble comb – here the galaxy type is linked to the nature and winding of the spiral arms which has been the primary criteria used to classify spiral galaxies over the last half century (Sandage 1961). Allowing for the varying spheroid-to-total ratio among each galaxy type, the Hubble grid helps to reveal how ellicular galaxies unify the early-type sequence and compare with late-type galaxies.

5 SUMMARY AND CONCLUSIONS

Early-type galaxies display a continuous distribution of spheroid-to-total flux ratios, going from disc-less, "pure" elliptical galaxies to disc-dominated lenticular galaxies

(Michard 1984; Djorgovski 1985; Carter 1987; Capaccioli 1987; Capaccioli et al. 1988; Franx et al. 1989; Nieto et al. 1988, 1991; Rix & White 1990, 1992; van den Bergh 1990; Bender 1990; Scorza & Bender 1990, 1995; Simien & Michard 1990; Cinzano & van der Marel 1993; D'Onofrio et al. 1995; Graham et al. 1998; Scorza 1998; Scorza & van den Bosch 1998; Bender & Saglia 1999)[4]. In between these two extremes lie galaxies with intermediate-scale discs, i.e. discs of kiloparsec-size that remain "embedded" within the spheroidal component of the galaxy and do not dominate the galaxy light at large radii as large-scale discs do. while this is likely known to some readers, the surge of papers presenting galaxy decompositions which are not aware of this reality has created a pressing need for this reminder. For ease of reference, we have introduced the term *ellicular* to designate such early-type galaxies with intermediate-scale discs. We have shown that the light distribution of ellicular galaxies can be accurately described with a simple spheroid + disc (+ optional nuclear component) model, without the need for the addition of a bright envelope-component.

Our decompositions correctly reproduce both the photometric (surface brightness and ellipticity profiles) and kinematic (specific angular momentum profile) properties of nine ellicular galaxies. Four of these nine ellicular galaxies (Mrk 1216, NGC 1271, NGC 1277, NGC 1332) and one additional elliptical galaxy (NGC 4291) had previously been claimed to be extreme outliers in the (black hole mass)-(spheroid mass) diagram. However, here we have demonstrated that, when correctly modelled, these five galaxies all reside well within the scatter of the correlation, i.e. they do not host overmassive black holes. This serves to strengthen the (black hole mass)-(spheroid mass) relation, and rules out the need for exotic formation scenarios.

6 ACKNOWLEDGMENTS

This research was supported by Australian Research Council funding through grant FT110100263. GS is grateful to Matteo Fossati, Luca Cortese and Giuseppe Gavazzi for useful comments and discussion. This work is based on observations made with the IRAC instrument (Fazio et al. 2004) on-board the Spitzer Space Telescope, which is operated by the Jet Propulsion Laboratory, California Institute of Technology under a contract with NASA, and also on observations made with the NASA/ESA Hubble Space Telescope, and obtained from the Hubble Legacy Archive, which is a collaboration between the Space Telescope Science Institute (STScI/NASA), the Space Telescope European Coordinating Facility (ST-ECF/ESA) and the Canadian Astronomy Data Centre (CADC/NRC/CSA). This research has made use of the GOLDMine database (Gavazzi et al. 2003) and the NASA/IPAC Extragalactic Database (NED) which is operated by the Jet Propulsion Laboratory, California Institute of Technology, under contract with the National Aeronautics and Space Administration.

[4] Many past studies were hampered by bulge/disc decompositions which forced an $R^{1/4}$ model for the bulge component and thus obtained spurious bulge-to-disc ratios, and from the *IRAF* task `ellipse` which does not report the correct deviations of isophotes from ellipses (Ciambur 2015).

REFERENCES

Allen P. D., Driver S. P., Graham A. W., Cameron E., Liske J., de Propris R., 2006, MNRAS, 371, 2
Arnold J. A., Romanowsky A. J., Brodie J. P., Chomiuk L., Spitler L. R., Strader J., Benson A. J., Forbes D. A., 2011, ApJ, 736, L26
Arnold J. A., et al., 2014, ApJ, 791, 80
Balcells M., Graham A. W., Peletier R. F., 2007, ApJ, 665, 1084
Barnes J. E., Hernquist L., 1992, Nature, 360, 715
Bender R., 1990, A&A, 229, 441
Bender R., Saglia R. P., 1999, in Merritt D. R., Valluri M., Sellwood J. A., eds, Astronomical Society of the Pacific Conference Series Vol. 182, Galaxy Dynamics - A Rutgers Symposium. p. 113 (arXiv:astro-ph/9811416)
Bogdán Á., et al., 2012, ApJ, 753, 140
Boroson T., 1981, ApJS, 46, 177
Capaccioli M., 1987, in de Zeeuw P. T., ed., IAU Symposium Vol. 127, Structure and Dynamics of Elliptical Galaxies. pp 47–60
Capaccioli M., Piotto G., Rampazzo R., 1988, AJ, 96, 487
Cappellari M., et al., 2011, MNRAS, 416, 1680
Carter D., 1987, ApJ, 312, 514
Ceverino D., Dekel A., Bournaud F., 2010, MNRAS, 404, 2151
Ceverino D., Dekel A., Mandelker N., Bournaud F., Burkert A., Genzel R., Primack J., 2012, MNRAS, 420, 3490
Ciambur B. C., 2015, preprint, (arXiv:1507.02691)
Cinzano P., van der Marel R. P., 1993, in Danziger I. J., Zeilinger W. W., Kjär K., eds, European Southern Observatory Conference and Workshop Proceedings Vol. 45, European Southern Observatory Conference and Workshop Proceedings. p. 105
Combes F., 2014a, preprint, (arXiv:1405.6405)
Combes F., 2014b, in Seigar M. S., Treuthardt P., eds, Astronomical Society of the Pacific Conference Series Vol. 480, Structure and Dynamics of Disk Galaxies. p. 211 (arXiv:1309.1603)
Conselice C., Mortlock A., Bluck A. F. L., 2012, in American Astronomical Society Meeting Abstracts 219. p. 107.04
D'Onofrio M., Zaggia S. R., Longo G., Caon N., Capaccioli M., 1995, A&A, 296, 319
Daddi E., et al., 2005, ApJ, 626, 680
Damjanov I., et al., 2009, ApJ, 695, 101
Danovich M., Dekel A., Hahn O., Teyssier R., 2012, MNRAS, 422, 1732
Dekel A., et al., 2009, Nature, 457, 451
Djorgovski S. B., 1985, PhD thesis, California Univ., Berkeley.
Driver S. P., Robotham A. S. G., Bland-Hawthorn J., Brown M., Hopkins A., Liske J., Phillipps S., Wilkins S., 2013, MNRAS, 430, 2622
Dullo B. T., Graham A. W., 2014, MNRAS, 444, 2700
Emsellem E., et al., 2011, MNRAS, 414, 888
Fazio G. G., et al., 2004, ApJS, 154, 10
Ferrarese L., et al., 2006, ApJS, 164, 334
Franx M., Illingworth G., Heckman T., 1989, ApJ, 344, 613
Gadotti D. A., 2008, MNRAS, 384, 420
Gavazzi G., Boselli A., Donati A., Franzetti P., Scodeggio M., 2003, A&A, 400, 451
Graham A. W., 2013, Elliptical and Disk Galaxy Structure and Modern Scaling Laws. p. 91, doi:10.1007/978-94-007-5609-0˙2
Graham A. W., 2014, in Seigar M. S., Treuthardt P., eds, Astronomical Society of the Pacific Conference Series Vol. 480, Structure and Dynamics of Disk Galaxies. p. 185 (arXiv:1311.7207)
Graham A. W., Worley C. C., 2008, MNRAS, 388, 1708
Graham A. W., Colless M. M., Busarello G., Zaggia S., Longo G., 1998, A&AS, 133, 325
Graham A. W., Erwin P., Trujillo I., Asensio Ramos A., 2003, AJ, 125, 2951
Graham A. W., Onken C. A., Athanassoula E., Combes F., 2011, MNRAS, 412, 2211

Graham A. W., Dullo B. T., Savorgnan G. A. D., 2015, ApJ, 804, 32
Head J. T. C. G., Lucey J. R., Hudson M. J., Smith R. J., 2014, MNRAS, 440, 1690
Hubble E. P., 1936, Realm of the Nebulae
Jedrzejewski R. I., 1987, MNRAS, 226, 747
Kent S. M., 1985, ApJS, 59, 115
Khochfar S., Silk J., 2006, ApJ, 648, L21
Kodaira K., Watanabe M., Okamura S., 1986, ApJS, 62, 703
Kormendy J., Bender R., 1996, ApJ, 464, L119
Kormendy J., Bender R., 2012, ApJS, 198, 2
Krajnović D., et al. 2013, MNRAS, 432, 1768
Läsker R., Ferrarese L., van de Ven G., 2014a, ApJ
Läsker R., Ferrarese L., van de Ven G., Shankar F., 2014b, ApJ
Laurikainen E., Salo H., Buta R., Knapen J. H., Comerón S., 2010, MNRAS, 405, 1089
Ledo H. R., Sarzi M., Dotti M., Khochfar S., Morelli L., 2010, MNRAS, 407, 969
Marconi A., Hunt L. K., 2003, ApJ, 589, L21
Martín-Navarro I., La Barbera F., Vazdekis A., Ferré-Mateu A., Trujillo I., Beasley M. A., 2015, MNRAS, 451, 1081
Martini P., Dicken D., Storchi-Bergmann T., 2013, ApJ, 766, 121
Meidt S. E., et al., 2014, ApJ, 788, 144
Méndez-Abreu J., CALIFA Team 2015, in Cenarro A. J., Figueras F., Hernández-Monteagudo C., Trujillo Bueno J., Valdivielso L., eds, Highlights of Spanish Astrophysics VIII. pp 268–273
Michard R., 1984, A&A, 140, L39
Michard R., Marchal J., 1993, A&AS, 98, 29
Moffat A. F. J., 1969, A&A, 3, 455
Navarro J. F., Benz W., 1991, ApJ, 380, 320
Nieto J.-L., Capaccioli M., Held E. V., 1988, A&A, 195, L1
Nieto J.-L., Bender R., Arnaud J., Surma P., 1991, A&A, 244, L25
Pastrav B. A., Popescu C. C., Tuffs R. J., Sansom A. E., 2013, A&A, 553, A80
Pichon C., Pogosyan D., Kimm T., Slyz A., Devriendt J., Dubois Y., 2011, MNRAS, 418, 2493
Prieto J., Jimenez R., Haiman Z., 2013, MNRAS, 436, 2301
Querejeta M., Eliche-Moral M. C., Tapia T., Borlaff A., Rodríguez-Pérez C., Zamorano J., Gallego J., 2015, A&A, 573, A78
Rest A., van den Bosch F. C., Jaffe W., Tran H., Tsvetanov Z., Ford H. C., Davies J., Schafer J., 2001, AJ, 121, 2431
Rix H.-W., White S. D. M., 1990, ApJ, 362, 52
Rix H.-W., White S. D. M., 1992, MNRAS, 254, 389
Rubin K. H. R., Prochaska J. X., Koo D. C., Phillips A. C., 2012, ApJ, 747, L26
Rusli S. P., Thomas J., Erwin P., Saglia R. P., Nowak N., Bender R., 2011, MNRAS, 410, 1223
Sandage A., 1961, The Hubble atlas of galaxies
Sandage A., 2005, ARA&A, 43, 581
Scorza C., 1998, in Aguilar A., Carraminana A., eds, IX Latin American Regional IAU Meeting, "Focal Points in Latin American Astronomy". p. 117
Scorza C., Bender R., 1990, A&A, 235, 49
Scorza C., Bender R., 1995, A&A, 293, 20
Scorza C., van den Bosch F. C., 1998, MNRAS, 300, 469
Scott N., Davies R. L., Houghton R. C. W., Cappellari M., Graham A. W., Pimbblet K. A., 2014, MNRAS, 441, 274
Sérsic J. L., 1963, Boletin de la Asociacion Argentina de Astronomia La Plata Argentina, 6, 41
Simien F., Michard R., 1990, A&A, 227, 11
Simien F., de Vaucouleurs G., 1986, ApJ, 302, 564
Stewart K. R., Brooks A. M., Bullock J. S., Maller A. H., Diemand J., Wadsley J., Moustakas L. A., 2013, ApJ, 769, 74
Trujillo I., et al., 2006, MNRAS, 373, L36
Ueda J., et al., 2014, ApJS, 214, 1
Walsh J. L., van den Bosch R. C. E., Gebhardt K., Yildirim A., Gültekin K., Husemann B., Richstone D. O., 2015, ApJ, 808, 183
White S. D. M., Frenk C. S., 1991, ApJ, 379, 52
White S. D. M., Rees M. J., 1978, MNRAS, 183, 341
Yıldırım A., van den Bosch R. C. E., van de Ven G., Husemann B., Lyubenova M., Walsh J. L., Gebhardt K., Gültekin K., 2015, MNRAS, 452, 1792
van Dokkum P. G., et al., 2008, ApJ, 677, L5
van den Bergh S., 1976, ApJ, 206, 883
van den Bergh S., 1990, ApJ, 348, 57
van den Bergh S., 1997, AJ, 113, 2054
van den Bosch R. C. E., Gebhardt K., Gültekin K., van de Ven G., van der Wel A., Walsh J. L., 2012, Nature, 491, 729